CrossMark

ORIGINAL PAPER

Modification of microcrystalline cellulose with pyridone derivatives for removal of cationic dyes from aqueous solutions

Chang Sun · Zhiyong Huang · Jiaxin Wang · Liming Rao ·
Jingjing Zhang · Jiao Yu · Jinmei Du · Changhai Xu

Abstract Microcrystalline cellulose (MCC) was modified with pyridone derivatives such as pyridone diester (PDE) and pyridone diacid (PDA) by using succinic acid anhydride as a linker. The modified MCCs were characterized by the fourier transform infrared spectroscopy, scanning electron microscopy, thermal gravimetric analysis, elemental analysis and solid state ^{13}C NMR. The adsorption capacities of the modified MCCs to cationic dyes were examined by using methylene blue (MB) as a model dye. It was found that the kinetic adsorption data followed the pseudo-second-order kinetic model, and the adsorption equilibriums were reached less than 10 min. The isothermal adsorption data were fitted with the Langmuir isotherm model very well, from which the maximum adsorption capacities of the MCCs modified with PDE and PDA were determined to be 101.01 and 142.86 mg/g, respectively. Further investigation showed that the modified MCCs were pH-dependent for adsorption of MB in aqueous solutions. The modified MCCs could be used for removal of MB from an aqueous solution at pH 8, and reused by regeneration in an acidic solution. It was tested that the modified MCCs had a high reusability for removal of MB from aqueous solutions, and still maintained high adsorption capacities even after multiple cycles of desorption–adsorption processes. Hence, the MCCs modified with PDE and PDA could be an effective and efficient approach to removal of cationic dyes from aqueous solutions.

Keywords Microcrystalline cellulose · Cellulose modification · Adsorption · Pyridone · Dye removal · Methylene blue

Introduction

Cellulose is the most abundant natural polymer in the world, and is being considered as one of the most promising adsorbents for removal of contaminant compounds in wastewaters because of its low cost, high biodegradability and renewability (Crini 2006; Forgacs et al. 2004; Gupta and Suhas 2009). The effluents discharged from the textile industries commonly contain a large amount of anionic dyes, cationic dyes or heavy metals. Hence, it is obligatory to remove these hazardous materials from the discharged effluents to mitigate the environmental impacts (Batmaz et al. 2014; Duan et al. 2013; Xiong et al. 2014). Cellulose could be functionalized with specific groups such as acids (Zhang et al. 2014; Zhou et al. 2013, 2014), ammonium or amine (Gurgel et al. 2009; Jin et al. 2015), imidazole (O'Connell et al. 2006) and calixarene (Tabakci et al. 2007) for efficient

C. Sun · Z. Huang · J. Wang · L. Rao ·
J. Zhang · J. Yu · J. Du · C. Xu (✉)
Key Laboratory of Eco-textiles, Ministry of Education,
College of Textiles and Clothing, Jiangnan University,
Wuxi 214122, Jiangsu, China
e-mail: changhai_xu@jiangnan.edu.cn

removal of anionic dyes, cationic dyes and heavy metals in effluents discharged from the textile industries. In our previous study, pyridone-based compounds were found to have good binding ability and selectivity towards heavy metals (Liu et al. 2015a, b). This inspires the current work, in which pyridone deriviaties such as pyridone diester (PDE) and pyridone diacid (PDA) were used for modification of microcrystalline cellulose (MCC), and the adsorption capacities of the modified MCCs to cationic dyes were investigated by using methylene blue (MB) as a model dye.
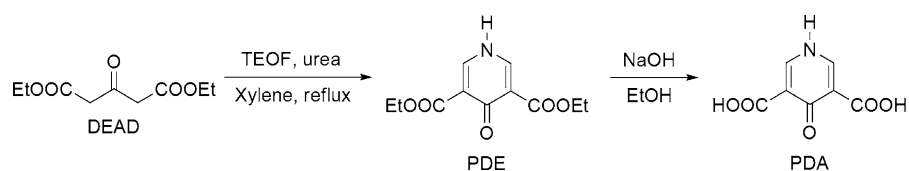
Experimental

Materials

MCC (50 μm) and triethyl orthoformate (TEOF) were purchased from J&K Scientific, China. Diethyl 1,3-acetonedicarboxylate (DEAD) was purchased from Shanghai DEMO Medical Teck Co., Ltd., China. Urea, succinic acid anhydride (SAA), methylene blue (MB) and 1,3-diisopropylcarbodiimide (DIC) were purchased from Sinopharm Chemical Regent Co., Ltd., China. All reagents were used without further purifications unless otherwise stated.

Synthesis of pyridone derivatives

The synthesis route for PDE and PDA is shown in Scheme 1. PDE was synthesized and purified in 75 % yield according to the method previously reported (Ren et al. 2011). PDE (9.56 g, 40.00 mmol) was dissolved in ethanol (100 mL) to which 1.0 M NaOH (80 mL) was added at room temperature. The reaction mixture was allowed to stir at room temperature overnight. Ethanol was removed in vacuo, and the aqueous solution was neutralized by the addition of 1.0 M HCl. The precipitated crude product was collected by filtration, and washed with ethanol to afford PDA as a white solid. MS–ESI: calculated for $[M]\text{-}(C_7H_4NO_5)$: m/z 182.1, found: m/z 182.1.

Modification of MCC with pyridone derivatives

The synthesis route for the modified MCC with PDE and PDA is shown in Scheme 2. MCC was firstly pretreated with SAA according to the method reported previously (Gurgel et al. 2008). 0.50 g of the SAA-pretreated MCC (SAA-MCC) was added to 50 mL of anhydrous dimethylformamide (DMF) containing 5 mL of DIC for reaction at room temperature for 1 h. 10 mmol of PDE or PDA was then added to the reaction solution in which an excess amount of PDE or PDA was used for the purpose to reduce the possibility of the formation of crosslinking. The reaction was maintained for 12 h at room temperature. The product was collected by filtration, and washed with DMF, ethanol and distilled water to afford the modified MCC in a white solid.

Characterization of modified MCCs

MS spectra were obtained on a Waters MALDI Synapt Q-TOF Mass Spectrometer. FTIR spectroscopy was performed on a Bruker Tensor 27 FTIR spectrometer. The morphologies of the modified MCCs were observed with a Hitachi SU-1510 scanning electron microscope (SEM) operated at 5 kV. Elemental analyses were performed on an Elementar Vario Micro select analyser. NMR experiments were performed with Bruker AVANCE III 200 and equipped with a 4.0 mm solid-state magic-angle-spinning (MAS) probe head. Thermal gravimetric analysis (TG) was performed using TA Instruments Q500 with a 100 mL/min flow of nitrogen. The TG curves were produced from 30 °C up to 500 °C at a heating rate of 10 °C/min.

Adsorption of the modified MCCs to MB

Adsorption kinetics

A sample of 25 mg of a modified MCC was added to 150 mL of an aqueous solution containing 20 mg/L MB. The adsorption was carried out at room

Scheme 1 Synthesis route to afford PDE and PDA
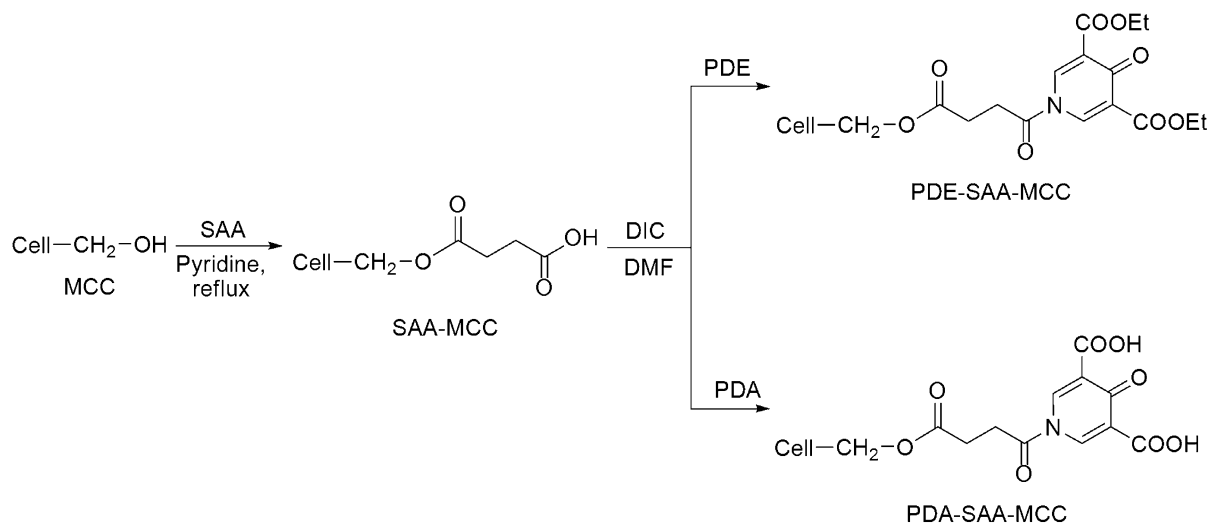
Scheme 2 Synthesis route to afford the modified MCCs with PDE and PDA

temperature under constant stirring. Aliquots of approximately 2.0 mL were taken at various intervals of time (t, min) during the adsorption process. After filtration, the concentrations of MB in solution (C_t, mg/L) were determined at the wavelength of its maximum absorbance (665 nm) in suitable diluted solutions by UV–Vis spectrometry, from which the adsorption capacity of MB on the modified MCC (q_t, mg/g) was calculated by the depletion of MB in solution as given in Eq. 1,

$$q_t = \frac{(C_0 - C_t)V}{m} \qquad (1)$$

where C_0 is the initial concentration of MB in the solution (mg/L), V is the volume of the solution (L), and m is the mass of the modified MCC (mg). All blanks and samples were run in triplicate to ensure reproducibility and accuracy. The kinetic adsorption curves were depicted by plotting q_t against t.

Adsorption isotherms

A sample of 25 mg of a modified MCC was added to 150 mL of an aqueous solution containing a specific concentration of MB ranging from 5 to 80 mg/L. The adsorption was carried out at room temperature under constant stirring. The concentration of MB in solution (C_e) and the adsorption capacity of MB on the modified MCC (q_e) at the equilibrium were determined by the methods as described above. The

isothermal adsorption curves were depicted by plotting q_e against C_e.

Effect of pH on the adsorption capacity of the modified MCCs to MB

The pH of the aqueous solution containing 20 mg/L MB was adjusted to a desired value by the dropwise addition of 0.1 M NaOH or HCl. A sample of 25 mg of a modified MCC was added to 150 mL of MB solution for adsorption under constant stirring at room temperature for 30 min. The adsorption capacities of MB on the modified MCC at various pH values were determined by Eq. (1).

Reusability of the modified MCCs for removal of MB

A sample of 25 mg of a modified MCC was added to 150 mL of MB solution at pH 8, and the adsorption was maintained under constant stirring at room temperature for 30 min. The adsorption capacity of MB on the modified MCC (q_0) was determined by Eq. (1). The sample of the modified MCC with a determined adsorption capacity of MB (q_0) was consecutively treated by multiple cycles of desorption–adsorption process as described below. The desorption process was carried out by adding the modified MCC saturated with MB to 150 mL of solution of 0.1 M HCl under constant stirring at room temperature for 4 h. After filtration and washing with

deionized water, the modified MCC was regenerated and dried in vacuum oven for reuse in a new cycle of adsorption. The adsorption capacity of MB on the modified MCC for this cycle of desorption–adsorption was noted as q_n (n = 1–5). The reusability of the modified MCC for removal of MB from aqueous solution was evaluated by the retention rate (R_n) of adsorption capacity of MB on the modified MCC in one cycle as calculated by Eq. (2).

$$R_n = \frac{q_n}{q_0} \times 100\,\% \qquad (2)$$

Results and discussion

### Modification of MCC with pyridone derivatives

As shown in Scheme 1, PDE was synthesized by the one-pot reaction of DEAD, TEOF and urea in xylene, from which PDA was prepared by hydrolysis in ethanol with the addition of sodium hydroxide. MCC was firstly pretreated with SAA, and then modified with PDE and PDA in DMF by using DIC as a coupling reagent (Scheme 2).

The modified MCCs were characterized by the FTIR spectroscopy as presented in Fig. 1. The major changes in FTIR spectrum for SAA-MCC in relation to MCC are the appearance of bands at 2933, 1720, 1646 and 1417 cm^{-1}. The band at 2933 cm^{-1} corresponds to asymmetric stretching of CH$_2$. The strong band at 1720 cm^{-1} corresponds to asymmetric and symmetric stretching of ester C=O. The bands at 1646

Fig. 1 FTIR spectra of the modified MCCs

and 1417 cm^{-1} corresponds to asymmetric and symmetric stretching of carboxylate ion, respectively. In comparison with the FTIR spectrum of SAA-MCC, the most relevant changes in the FTIR spectrum of the PDE-SAA-MCC are the appearance of bands at 2979, 1703 and 1646 cm^{-1}. The broad band at 2979 cm^{-1} corresponds to symmetric and asymmetric vibrations of the ethyl group introduced from PDE. The band at 1703 cm^{-1} corresponds to stretching vibration of carbonyl groups such as ester, amide and ketone. The band at 1646 cm^{-1} corresponds to the stretching vibration of C=C in the pyridone group. This indicates that PDE was successfully coupled with the SAA-MCC. In the FTIR spectrum of the PDA-SAA-MCC, it was found that the band at 2979 cm^{-1} disappeared and a weak broad band around 3328 cm^{-1} appeared due to the fact that the ethyl ester in PDE was hydrolyzed to its corresponding acid.

The FTIR spectra could be used as an indication of the adsorption mode of MB on the modified MCCs. It can be seen from Fig. 2a that bands at 3208 and 1727 cm^{-1} corresponding to –OH and C=O of PDA-SAA-MCC shift to 3400 and 1753 cm^{-1} after adsorption, suggesting that these groups involved in the interaction of PDA-SAA-MCC and MB. The appearance of band at 1604 cm^{-1} corresponding to C=N vibration, band at 1398 cm^{-1} corresponding to symmetric C–N stretch and band at 1354 cm^{-1} corresponding to symmetric –CH$_3$ deformation after adsorption suggested that the surface of PDA-SAA-MCC was coated with MB. No significant peak is found in Fig. 2b for PDE-SAA-MCC after adsorption except a weak peak at 1398 cm^{-1} corresponding to symmetric C–N stretch of MB as most of the typical adsorption bands of the dye were overlapped with those of PDE-SAA-MCC. Because of the relatively weak interaction between PDE-SAA-MCC and MB, no obvious band shifts were observed after adsorption.

Figure 3 shows the surface morphologies of the modified MCCs. It can be seen that the consecutive modifications with SAA, PDE and PDA made the surface of MCC much rougher. Especially, the modified MCCs exhibited an increased particle size compared to MCC, which may be attributed to the introduction of pyridone functional groups as well as the modification process. Hence, the modified MCCs possessed a fractured and loose surface structure and as such an enlarged specific surface area that would be favorable for dye adsorption.
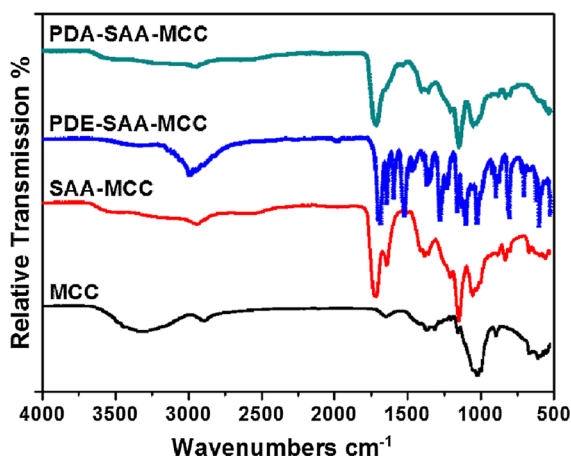
Fig. 2 FTIR spectra of
a PDA-SAA-MCC + MB
and b PDE-SAA-
MCC + MB
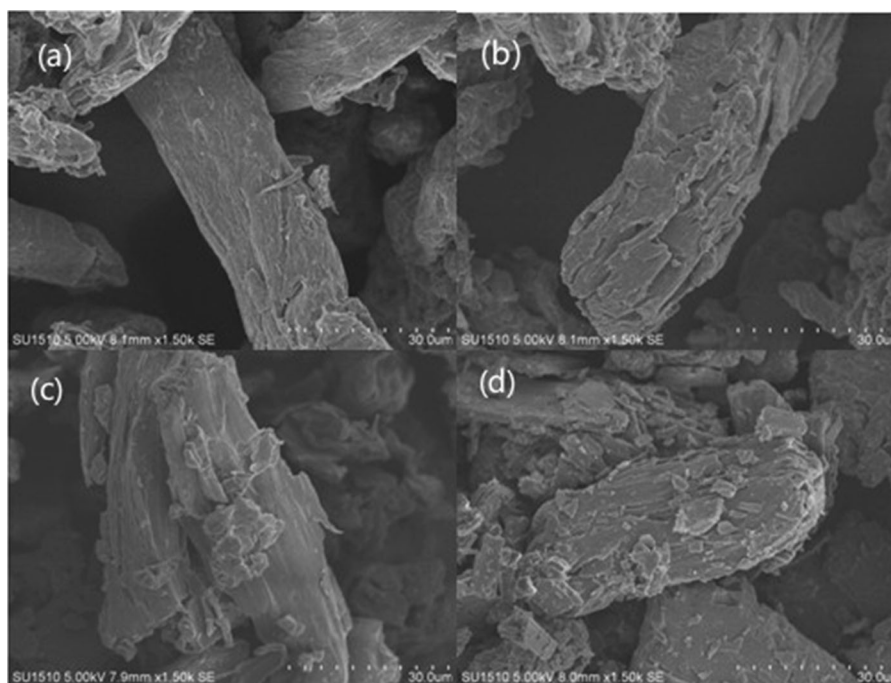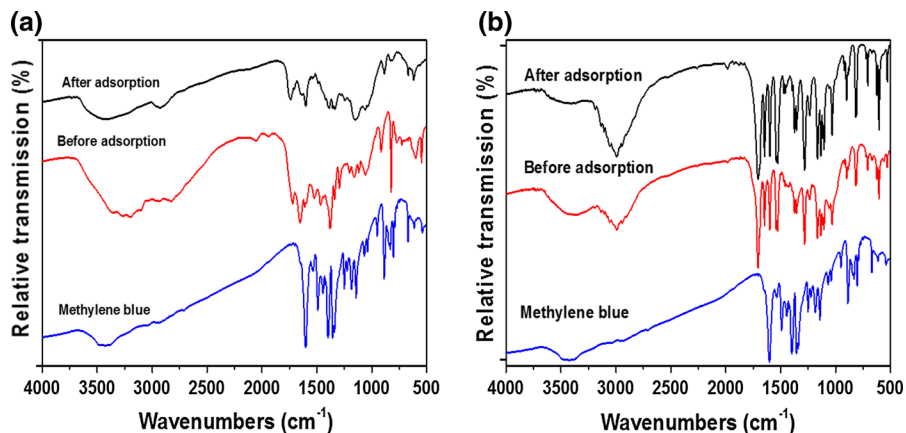
Fig. 3 SEM images of a MCC, b SAA-MCC, c PDE-SAA-MCC and d PDA-SAA-MCC

The elemental analysis results given in Table 1 confirmed that the modification of MCC was accomplished. The amounts of the bonded functional groups were calculated according to the contents of C in SAA-MCC, or N in PDE-SAA-MCC and PDA-SAA-MCC. The structures of prepared materials were also confirmed by solid-state ^{13}C NMR spectra shown in Fig. 4 with assignment. Four partially overlapping peaks were found in the anhydroglucose carbon region of SAA-MCC spectra at 101.0, 88.2, 72.9 and 63.0 ppm correspond to C_1, C_4, $C_{2,\ 3,\ 5}$ and C_6,

respectively. Two more peaks compared to native cellulose spectra were found at 173.5 and 29.1 ppm corresponding to carbonyl and methylene carbons of the succinic group. The doublet splitting in the carbonyl and/or ethyl carbon region of PDE-SAA-MCC and PDA-SAA-MCC could be explained by the presence of two crystalline allomorphs of these materials. The major difference in the spectra of PDE-SAA-MCC and PDA-SAA-MCC is that the former one exhibits resonance of ethyl carbon at 63.1, 60.6, 14.8 and 13.5 ppm.

Table 1 Results of elemental analysis for MCC, SAA-MCC, PDE-SAA-MCC and PDA-SAA-MCC

| Samples	%N	%C	%H	Bonded amount (mmol/g)
MCC	0.1	41.86	6.839	–
SAA-MCC	0.12	43.56	5.773	2.77
PDE-SAA-MCC	4.89	52.68	6.119	3.49
PDA-SAA-MCC	4.04	44	4.548	2.88
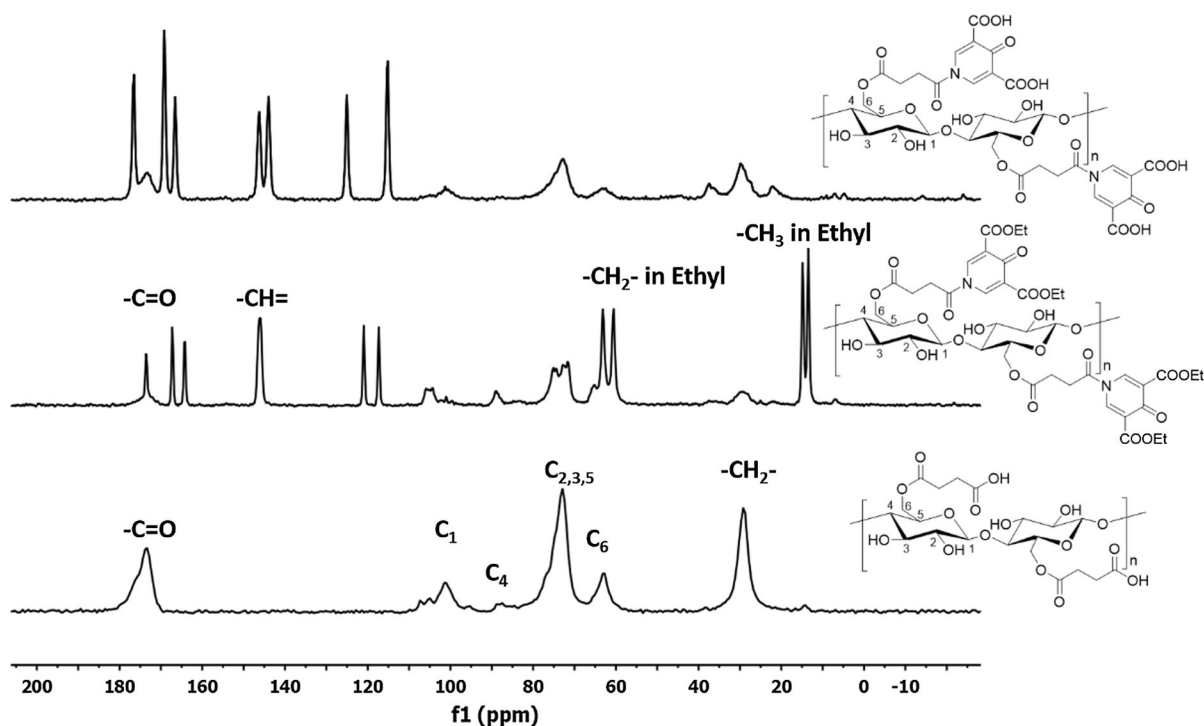
Fig. 4 Solid-state ^{13}C NMR spectra of PDA-SAA-MCC, PDE-SAA-MCC and SAA-MCC

Thermogravimetric curves of the modified MCCs are shown in Fig. 5. Three distinct zones were shown in the TG curves. Slight weight loss in the initial zone occurred due to the evaporation of absorbed water. At the second stage, rapid weight loss was found because of the pyrolysis reaction which may cause the break of chemical bonds within the materials and as such rapid decrease in degree of polymerization. The maximum weight loss rate for MCC, SAA-MCC, PDE-SAA-MCC and PDA-SAA-MCC were found to be 2.48 wt%/°C at 349 °C, 0.84 wt%/°C at 308 °C, 1.67 wt%/°C at 259 °C and 2.93 wt%/°C at 311 °C, respectively. The results are coincident with previous report that organically modified cellulose undergoes thermal decomposition at lower temperatures

compared to the native one (Gurnani et al. 2003). The small curvatures observed from Fig. 5 for PDE-SAA-MCC and PDA-SAA-MCC were most likely ascribed to the formation and evaporation of decomposition products. Finally, the decomposition rate gradually decreased to a constant weight at around 400 °C.

Figure 6 shows the thermal properties of the modified MCCs with MB. It can be seen from the TG curves that the weight loss rate decreased, and the mass loss ratio reduced from 90 to 44 % for PDA-SAA-MCC and 97–88 % for PDE-SAA-MCC, respectively. This is probably due to the fact that the dye has a high carbon content than the modified MCCs. A well-defined mass loss was found over the

Fig. 5 TG and DTG curves of **a** MCC, **b** SAA-MCC, **c** PDE-SAA-MCC and **d** PDA-SAA-MCC
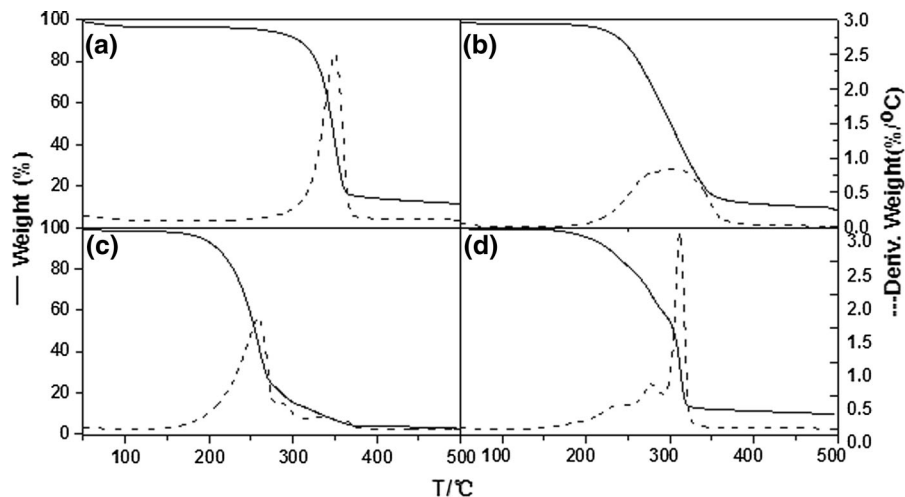
Fig. 6 TG curve of **a** PDA-SAA-MCC + MB and **b** PDE-SAA-MCC + MB
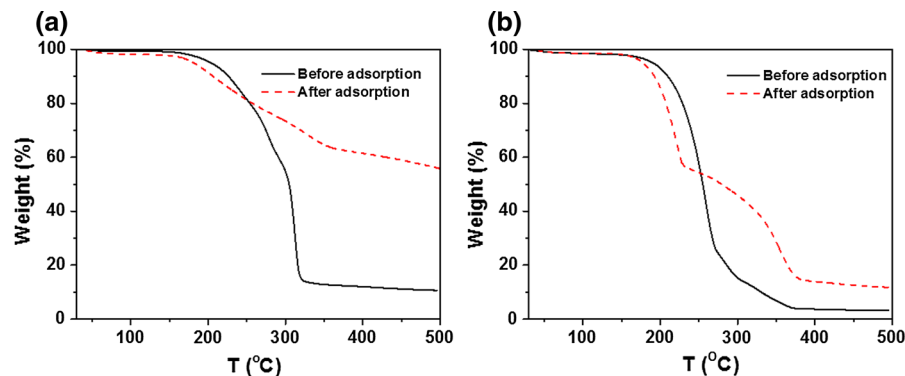
temperature ranging from 230 to 480 °C corresponding to the thermodesorption of adsorbed MB in PDE-SAA-MCC system, while no thermodesorption curve was found in the PDA-SAA-MCC system as the binding force between PDA-SAA-MCC and MB is stronger than that of PDE-SAA-MCC system.

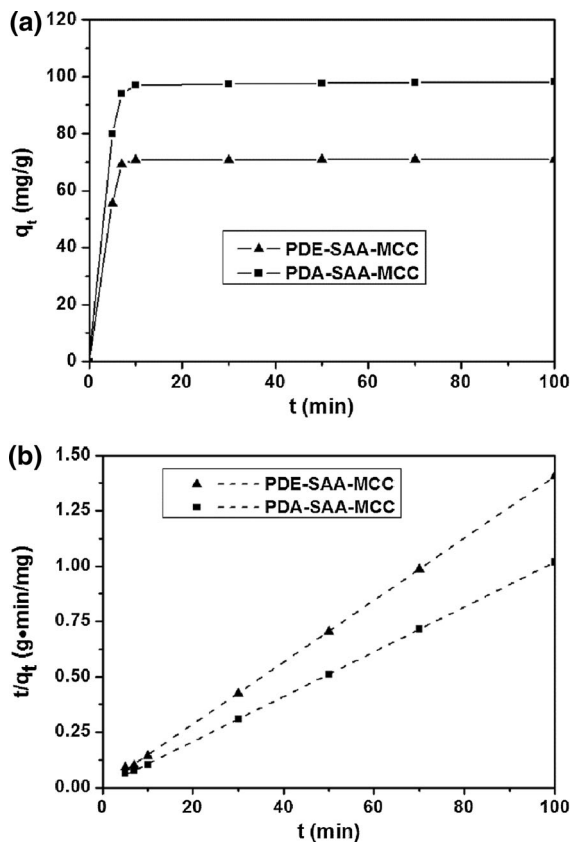Adsorption of MB on the modified MCCs

Adsorption kinetics

The kinetic adsorption curves of MB on MCCs modified with PDE and PDA are shown in Fig. 7a. It can be seen that both PDE-SAA-MCC and PDA-SAA-MCC exhibited rapid adsorption to MB, and the adsorption equilibrium was achieved within 10 min. This is mainly due to the fact that the modified MCCs had a large number of available binding sites which were responsible for the relatively strong interaction with MB. No significant change in adsorption capacity

was found in the time range of 10–100 min as the binding sites were fully occupied by MB. It appears in Fig. 7a that PDA-SAA-MCC had a higher adsorption capacity than PDE-SAA-MCC. This is mainly because PDA-SAA-MCC was derived from PDE-SAA-MCC by hydrolysis, and thus possessed a highly negatively-charged surface which would produce a relatively strong electrostatic attractive force to cationic MB.

The kinetic adsorption data shown in Fig. 7a were fitted to various kinetic models, and were found to follow the pseudo-second-order kinetic model as given by Eq. (3),

$$\frac{t}{q_t} = \frac{1}{kq_e^2} + \frac{t}{q_e} \tag{3}$$

where q_t (mg/g) is the adsorption capacity of MB on the modified MCCs at a time interval (t, min), q_e (mg/g) is the equilibrium adsorption capacity of MB on the modified MCCs, and k is the equilibrium rate constant.

Fig. 7 Kinetic adsorption curves of **a** MB on MCCs modified with PDE and PDA and **b** the linear regression plots for the pseudo-second-order kinetic model

Table 2 Results of linear regression for the pseudo-second-order kinetic model for describing the kinetic adsorption of MB on the modified MCCs

Modified MCC	q_e, mg/g	k, g/(mg min)	R^2
PDE-SAA-MCC	71.53	0.0258	0.9998
PDA-SAA-MCC	98.72	0.0135	0.9999

effective and efficient for adsorption of MB than PDE-SAA-MCC.

Considering the rapid adsorption of MB on the modified MCCs, an adsorption process for a period of 30 min would be adequate in the current work for further investigations.
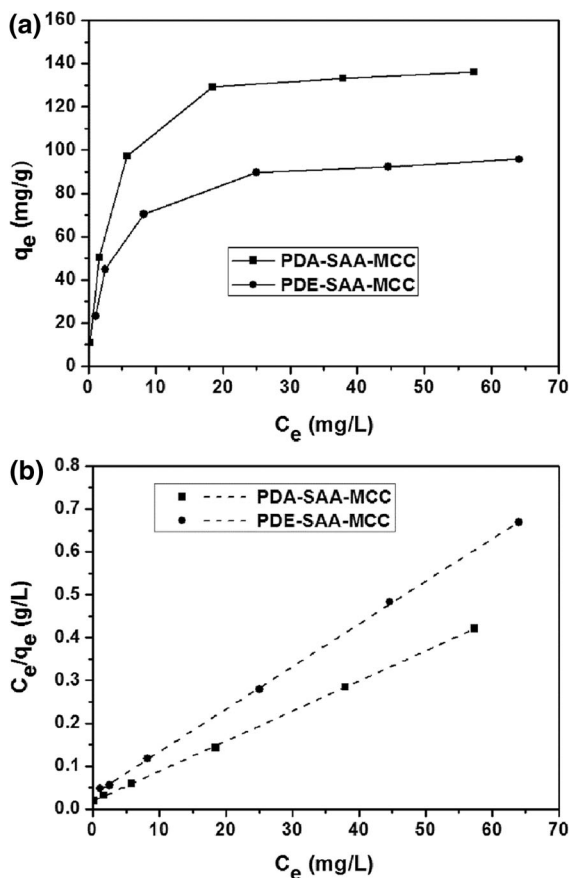
Adsorption isotherms equilibrium

To understand the interactions of the modified MCCs with MB, the isothermal adsorption data were plotted as shown in Fig. 8a. The model fitting study suggested that the isothermal adsorption data shown in Fig. 8a followed the Langmuir isotherm model as given in Eq. (4),

$$\frac{C_e}{q_e} = \frac{1}{Kq_m} + \frac{C_e}{q_m} \qquad (4)$$

where q_e (mg/g) is the equilibrium adsorption capacity of MB on the modified MCC, C_e (mg/L) is the equilibrium concentration of MB in solution, q_m (mg/g) is the maximum equilibrium adsorption capacity of MB on the modified MCC, and K (L/mg) is the Langmuir adsorption equilibrium constant related to the affinity of binding sites. Figure 8b shows the Langmuir isotherm plots for adsorption of MB on the modified MCCs, from which q_m and K were calculated as summarized in Table 3.

As can be seen in Table 3, the squared correlation coefficients (R^2) produced by the linear regression are much close to unity. This indicates that the adsorption of MB on the modified MCCs could be well described by the Langmuir isotherm model. PDA-SAA-MCC exhibited a much greater q_m to MB than PDE-SAA-MCC. This can be attributed to the fact that the carboxylate groups in PDA-SAA-MCC provide more binding sites for MB adsorption while PDE-SAA-MCC is lack of negatively-charged functional groups. Hence, PDA-SAA-MCC could be more applicable for

The linear regression plots for the pseudo-second-order kinetic model is shown in Fig. 7b, from which the kinetic adsorption parameters were calculated as summarized in Table 2.

As can be seen in Table 2, the equilibrium adsorption capacities of MB on the modified MCCs determined by the pseudo-second-order kinetic model were in a good agreement with the experimentally observed data (Fig. 7a), and the squared correlation coefficients (R^2) were found to be much close to unity. These results confirmed that the kinetic adsorption of MB on the modified MCCs could be well described by the pseudo-second-order kinetic model, and the rate-limiting step may be chemisorption (Ho and McKay 1998). In addition, PDA-SAA-MCC was found to have a greater equilibrium adsorption capacity and a lower equilibrium rate constant than PDE-SAA-MCC. This indicates that PDA-SAA-MCC was more

Fig. 8 Adsorption isotherms of **a** MB on the modified MCCs, and **b** the Langmuir isotherm plots for adsorption of MB on the modified MCCs

adsorption of cationic dyes than PDE-SAA-MCC (Table 3).

Table 4 shows a comparative assessment of methane blue adsorption capacities on various cellulose-based adsorbents. It can be seen that PDA-SAA-MCC presented higher adsorption capacity than hydroxypropyl cellulose hydrogel, nanocrystalline, nanofibrils cellulose or its precursor, i.e. SAA-MCC and PDE-SAA-MCC while it presented moderate

Table 3 Results of linear regression for the Langmuir adsorption model for describing the equilibrium adsorption of MB on the modified MCCs

Modified MCC	q_m, mg/g	K, L/mg	R^2
PDE-SAA-MCC	100.50	0.29	0.9997
PDA-SAA-MCC	142.65	0.38	0.9997

adsorption efficiency compared with most of the cellulosic nano-materials.

Effect of pH on the adsorption capacity of MB on the modified MCCs

The modified MCCs were examined for adsorption of MB in aqueous solutions at various pH values. Figure 9 shows the effect of pH on the adsorption capacity of MB on the modified MCCs. It was found that the adsorption capacities of MB on PDE-SAA-MCC and PDA-SAA-MCC increased as pH increased and reached the maximum values at pH 8. This is mainly because the functional groups in the modified MCCs were readily protonated at a lower pH, thereby resulting in the reduction of negative charges in the modified MCCs which play a dominant role in the adsorption of MB. As pH increased to 8, however, the protonated functional groups were gradually neutralized and negatively-charged binding sites were optimally formed on the modified MCCs which produced strong electrostatic attraction to MB. It is interesting that the adsorption capacities of the modified MCCs slightly decreased as pH increased from 8 to 10, for which a possible reason is that the positive charge of MB would be diminished under relatively strong alkaline conditions. Additionally, it was found in Fig. 9 that PDA-SAA-MCC was more susceptible to pH than PDE-SAA-MCC for adsorption of MB probably due to the fact that PDA-SAA-MCC contains a number of functional groups which can be switched between COOH and COO^- by protonation and deprotonation.

Reusability of the modified MCCs for removal of MB from aqueous solution

The pH-dependence of the modified MCCs for adsorption of MB shown in Fig. 9 indicates that the modified MCCs can be reused for removal of MB from aqueous solution by regenerating the modified MCCs in acidic solutions. In order to examine the reusability, five cycles of desorption–adsorption processes were consecutively carried on a modified MCC sample on which MB was initially adsorbed, and the retention rate (R_n) of adsorption capacity of MB on the modified MCC in each cycle of desorption–adsorption process was determined as given in Table 5. As can be seen in Table 5, the retention rate of adsorption capacity of

Table 4 Adsorption capabilities of MCCs modified with PDE and PDA compared with other cellulosic adsorbents

Adsorbents	Q_{max} (mg/g)	References
Carboxymethyl cellulose	223	Yan et al. (2011)
Cellulose nanocrystals	769	Batmaz et al. (2014)
Hydroxypropyl cellulose hydrogel composited with graphene oxide	118.4	Liu et al. (2015a, b)
Carboxylate-functionalized cellulose nanocrystals	243.9	Qiao et al. (2015)
Cellulose nanocrystal-alginate hydrogel beads	256.41	Mohammed et al. (2015)
Cellulose nanofibrils	122.2	Chan et al. (2015)
Nanocrystalline cellulose	101	He et al. (2013)
SAA-MCC	81.4	This work
PDE-SAA-MCC	100.50	This work
PDA-SAA-MCC	142.86	This work
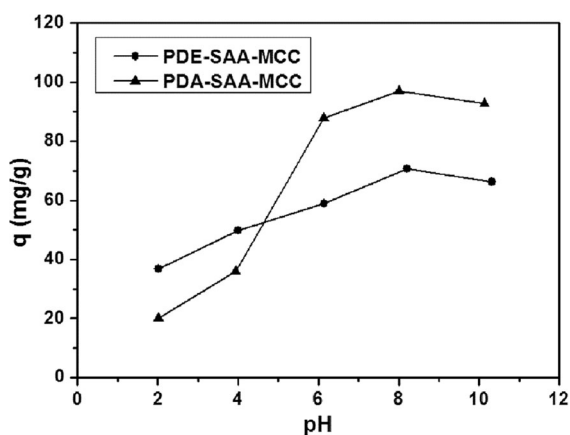
Fig. 9 Effect of pH on adsorption of MB on the modified MCCs

Table 5 Retention rate of adsorption capacities of the modified MCCs to MB for various cycles of reuse

Modified MCC	R_0 (%)	R_1 (%)	R_2 (%)	R_3 (%)	R_4 (%)	R_5 (%)
PDE-SAA-MCC	100	97	93	91	80	75
PDA-SAA-MCC	100	99	96	95	93	87

MB on the modified MCC decreased gradually with an increasing cycle number of the desorption–adsorption process. However, with five cycles of desorption–adsorption processes, PDA-SAA-MCC had its adsorption capacity only decreased by 13 %, and PDE-SAA-MCC by 25 %. This indicates that the modified MCCs had a high reusability for removal of MB from aqueous solution, and could be simply regenerated in an acidic solution for reuse.

Conclusions

MCC was successfully modified with PDE and PDA, and the modified MCCs were found to exhibit a loose and fractured morphology which would benefit to adsorption of cationic dyes in aqueous solutions. The results of kinetic adsorption experiment revealed that the adsorption of MB on the modified MCCs followed the pseudo-second-order kinetic model, and the adsorption equilibriums were reached less than 10 min. The equilibrium adsorption of MB on the modified MCCs could be well described by the Langmuir isotherm model. The adsorption of MB on the modified MCCs were pH-dependent, which made it feasible that the modified MCCs could be used for optimally removing MB from an aqueous solution at pH 8, and be regenerated in an acidic solution for reuse. It was indicated by multiple cycles of desorption–adsorption process that the modified MCCs had a high reusability for removal of cationic dyes such as MB from aqueous solutions.

References

Batmaz R, Mohammed N, Zaman M, Minhas G, Berry RM, Tam KC (2014) Cellulose nanocrystals as promising adsorbents for the removal of cationic dyes. Cellulose 21:1655–1665

Chan CH, Chia CH, Zakaria S, Sajab MS, Chin SX (2015) Cellulose nanofibrils: a rapid adsorbent for the removal of methylene blue. RSC Adv 5:18204–18212

Crini G (2006) Non-conventional low-cost adsorbents for dye removal: a review. Bioresour Technol 97:1061–1085

Duan C, Zhao N, Yu X, Zhang X, Xu J (2013) Chemically modified kapok fiber for fast adsorption of Pb^{2+}, Cd^{2+}, Cu^{2+} from aqueous solution. Cellulose 20:849–860

Forgacs E, Cserháti T, Oros G (2004) Removal of synthetic dyes from wastewaters: a review. Environ Int 30:953–971

Gupta VK, Suhas (2009) Application of low-cost adsorbents for dye removal – a review. J Environ Manag 90:2313–2342

Gurgel LVA, Júnior OK, Gil RPF, Gil LF (2008) Adsorption of Cu(II), Cd(II), and Pb(II) from aqueous single metal solutions by cellulose and mercerized cellulose chemically modified with succinic anhydride. Bioresour Technol 99:3077–3083

Gurgel LVA, Perin de Melo JC, de Lena JC, Gil LF (2009) Adsorption of chromium (VI) ion from aqueous solution by succinylated mercerized cellulose functionalized with quaternary ammonium groups. Bioresour Technol 100:3214–3220

Gurnani V, Singh AK, Venkataramani B (2003) Cellulose based macromolecular chelator having pyrocatechol as an anchored ligand: synthesis and applications as metal extractant prior to their determination by flame atomic absorption spectrometry. Talanta 61:889–903

He X, Male KB, Nesterenko PN, Brabazon D, Paull B, Luong JHT (2013) Adsorption and desorption of methylene blue on porous carbon monoliths and nanocrystalline cellulose. ACS Appl Mater Interfaces 5:8796–8804

Ho YS, McKay G (1998) A comparison of chemisorption kinetic models applied to pollutant removal on various sorbents. Process Saf Environ 76:332–340

Jin L, Li W, Xu Q, Sun Q (2015) Amino-functionalized nanocrystalline cellulose as an adsorbent for anionic dyes. Cellulose 22:2443–2456

Liu X, Zhou Y, Nie W, Song L, Chen P (2015a) Fabrication of hydrogel of hydroxypropyl cellulose (HPC) composited with graphene oxide and its application for methylene blue removal. J Mater Sci 50:6113–6123

Liu Y, Shen J, Sun C, Ren C, Zeng H (2015b) Intramolecularly hydrogen-bonded aromatic pentamers as modularly tunable macrocyclic receptors for selective recognition of metal ions. J Am Chem Soc 137:12055–12063

Mohammed N, Grishkewich N, Berry RM, Tam KC (2015) Cellulose nanocrystal–alginate hydrogel beads as novel adsorbents for organic dyes in aqueous solutions. Cellulose 22:3725–3738

O'Connell DW, Birkinshaw C, O'Dwyer TF (2006) A chelating cellulose adsorbent for the removal of Cu(II) from aqueous solutions. J Appl Polym Sci 99:2888–2897

Qiao H, Zhou Y, Yu F, Wang E, Min Y, Huang Q, Pang L, Ma T (2015) Effective removal of cationic dyes using carboxylate-functionalized cellulose nanocrystals. Chemosphere 141:297–303

Ren C, Maurizot V, Zhao H, Shen J, Zhou F, Ong WQ, Du Z, Zhang K, Su H, Zeng H (2011) Five-fold-symmetric macrocyclic aromatic pentamers: high-affinity cation recognition, ion-pair-induced columnar stacking, and nanofibrillation. J Am Chem Soc 133:13930–13933

Tabakci M, Erdemir S, Yilmaz M (2007) Preparation, characterization of cellulose-grafted with calix[4]arene polymers for the adsorption of heavy metals and dichromate anions. J Hazard Mater 148:428–435

Xiong J, Jiao C, Li C, Zhang D, Lin H, Chen Y (2014) A versatile amphiprotic cotton fiber for the removal of dyes and metal ions. Cellulose 21:3073–3087

Yan H, Zhang W, Kan X, Dong L, Jiang Z, Li H, Yang H, Cheng R (2011) Sorption of methylene blue by carboxymethyl cellulose and reuse process in a secondary sorption. Colloids Surf A 380:143–151

Zhang G, Yi L, Deng H, Sun P (2014) Dyes adsorption using a synthetic carboxymethyl cellulose-acrylic acid adsorbent. J Env Sci 26:1203–1211

Zhou Y, Zhang M, Hu X, Wang X, Niu J, Ma T (2013) Adsorption of cationic dyes on a cellulose-based multi-carboxyl adsorbent. J Chem Eng Data 58:413–421

Zhou Y, Zhang M, Wang X, Huang Q, Min Y, Ma T, Niu J (2014) Removal of crystal violet by a novel cellulose-based adsorbent: comparison with native cellulose. Ind Eng Chem Res 53:5498–5506